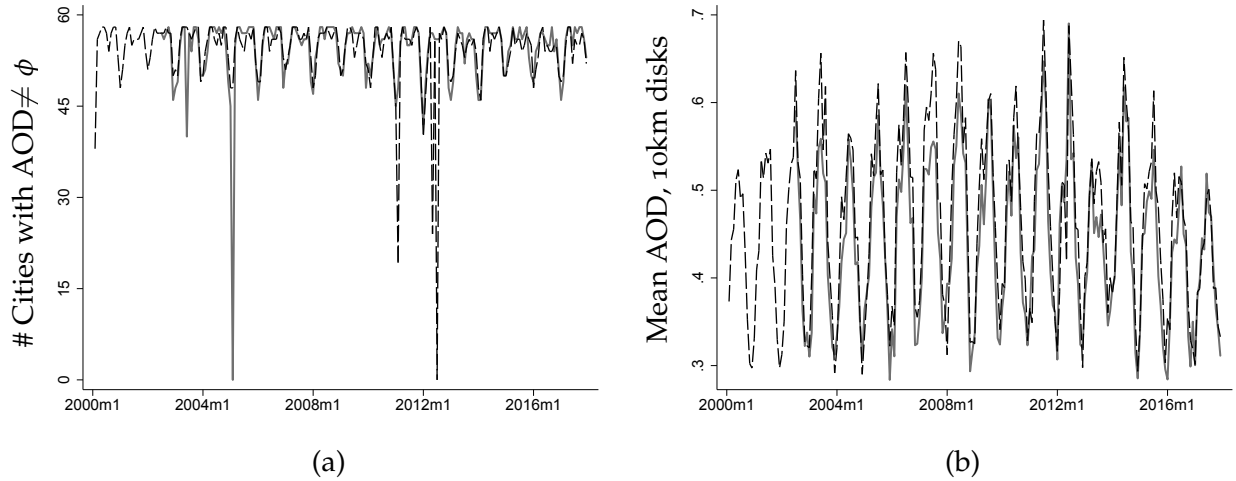


# Online Appendix for “Subways and Urban Air Pollution” by Gendron-Carrier, Gonzalez-Navarro, Polloni and Turner

## A AOD data

Figure A.1: MODIS Terra and Aqua AOD data



Note: Panel (a) gives count of new subway cities in our primary estimation sample with non-missing AOD 10km measurements by month for Terra (dashed black) and Aqua (gray). Panel (b) shows mean AOD within 10km of the center of subway cities, averaged over cities, by month for Terra (dashed black) and Aqua (gray).

The Moderate Resolution Imaging Spectroradiometers (MODIS) aboard the Terra and Aqua Earth observing satellites measure the ambient aerosol optical depth (AOD) of the atmosphere almost globally. We use MODIS Level-2 daily AOD products from Terra for February 2000-December 2017 and Aqua for July 2002-December 2017 to construct monthly average AOD levels in cities. We download all the files from the NASA File Transfer Protocol.<sup>1</sup>

There are four MODIS Aerosol data product files: *MOD04\_L2* and *MOD04\_3K*, containing data collected from the Terra platform; and *MYD04\_L2* and *MYD04\_3K*, containing data collected from the Aqua platform. We use products *MOD04\_3K* and *MYD04\_3K* to get AOD measures at a spatial resolution (pixel size) of approximately 3 x 3 kilometers. Each product file covers a five-minute time interval based on the start time of each MODIS granule. The product files are stored in Hierarchical Data Format (HDF) and we use the "Optical Depth Land And Ocean" layer, which is stored as a Scientific Data Set (SDS) within the HDF file, as our measure of aerosol optical depth. The "Optical Depth Land And Ocean" dataset contains only the AOD retrievals of high quality.

We convert all HDF formatted granules to GIS compatible formats using the HDF-EOS To GeoTIFF Conversion Tool (HEG) provided by NASA's Earth Observing System Program.<sup>2</sup> We consolidate GeoTIFF granules into a global raster for each day using ArcGIS. First, we keep only AOD values that do contain information. The missing value is -9999 in AOD retrievals. Second, we create a raster catalog with all the granules for a given day and calculate the average AOD value using the Raster Catalog to Raster Dataset tool.

<sup>1</sup><ftp://ladsweb.nascom.nasa.gov/allData/6/>

<sup>2</sup>The most recent version of the software, HEG Stand-alone v2.13, can be downloaded at <http://newsroom.gsfc.nasa.gov/sdptoolkit/HEG/HEGDownload.html>

Figure A.1 provides more information about the coverage of the two satellites and the prevalence of missing data. The black dashed line in panel (a) of the figure gives the count of cities in our primary estimation sample for which we calculate an AOD from the Terra satellite reading for each month of our study period. These are cities for which there is at least one pixel within 10km of the center on one day during the relevant month. Since most of the cities in our data are in the Northern hemisphere, we see a strong seasonal pattern in this series. The light gray line in this figure reports the corresponding quantity calculated from the Aqua satellite reading. Since Aqua became operational after Terra, the Aqua series begins later. The Aqua satellite data tracks the Terra data closely, but at a slightly lower level. Panel (b) of Figure A.1 reports city mean AOD data for all city-months in our sample over the course of our study period. As for the other series, this one too exhibits seasonality, although this will partly reflect a composition effect. As we see in panel (a) not all cities are in the data for all months. As in the first two panels, the dark line describes AOD readings from Terra and the light gray, Aqua.

## **B Ridership data**

We gathered subway ridership data (unlinked trips) for 42 of the subway systems in our main estimating sample, mostly from annual reports or statistical agencies. In 16 cases we were either not able to find data on ridership at all, the data were not available from the opening date, or the ridership data was aggregated across cities or other rail systems. Data sources for each of the cities we were able to obtain usable data are detailed in Table A.1.

Table A.1: Ridership Data Sources

City	Source & URL	Date accessed
Almaty (Kazakhstan)	International Metro Association reports <a href="http://eng.asmetro.ru/metro/techno_ekonom/">http://eng.asmetro.ru/metro/techno_ekonom/</a>	Feb. 2020
Bangalore (India)	Bangalore Metro operational performance reports <a href="https://kannada.bmrc.co.in/English/rti.html">https://kannada.bmrc.co.in/English/rti.html</a>	Feb. 2020
Brescia (Italy)	Brescia Mobilitá reports <a href="https://www.comune.brescia.it">https://www.comune.brescia.it</a>	Feb. 2020
Changsha (China)	China Association of Metros annual reports <a href="https://www.camet.org.cn/tjxx/3101">https://www.camet.org.cn/tjxx/3101</a>	Feb. 2020
Chennai (India)	Chennai Metro Rail Limited annual reports <a href="https://chennaimetrorail.org">https://chennaimetrorail.org</a>	Feb. 2020
Copenhagen (Denmark)	Statistics Denmark <a href="https://www.statbank.dk/bane21">https://www.statbank.dk/bane21</a>	Feb. 2020
Daejeon (South Korea)	Daejeon Metropolitan Rapid Transit Corporation <a href="http://info.korail.com/common/download.mbs?fileSeq=14648002&amp;boardId=9863289">http://info.korail.com/common/download.mbs?fileSeq=14648002&amp;boardId=9863289</a>	Feb. 2020
Delhi (India)	Delhi Metro Rail Corporation annual reports <a href="http://www.delhimetrorail.com/annual_report.aspx">http://www.delhimetrorail.com/annual_report.aspx</a>	Feb. 2020
Dongguan (China)	China Association of Metros annual reports <a href="https://www.camet.org.cn/tjxx/3101">https://www.camet.org.cn/tjxx/3101</a>	Feb. 2020
Dubai (UAE)	Dubai Road and Transport Auth.: Annual statistical reports <a href="https://www.dsc.gov.ae/Report/Copy%20of%20DSC_SYB_2016_11%20_%2011.xlsx">https://www.dsc.gov.ae/Report/Copy%20of%20DSC_SYB_2016_11%20_%2011.xlsx</a>	Feb. 2020
Fuzhou (China)	China Association of Metros annual reports <a href="https://www.camet.org.cn/tjxx/3101">https://www.camet.org.cn/tjxx/3101</a>	Feb. 2020
Gwangju (South Korea)	Gwangju Subway reports <a href="http://info.korail.com/common/download.mbs?fileSeq=14648002&amp;boardId=9863289">http://info.korail.com/common/download.mbs?fileSeq=14648002&amp;boardId=9863289</a>	Feb. 2020
Hangzhou (China)	Hangzhou Statistical Yearbook	Feb. 2020

Continued on next page

**Table A.1 – continued from previous page**

City	Source & URL	Date accessed
Harbin (China)	<a href="https://www.camet.org.cn/tjxx/3101">https://www.camet.org.cn/tjxx/3101</a> China Association of Metros annual reports	Feb. 2020
Jaipur (India)	<a href="https://www.camet.org.cn/tjxx/3101">https://www.camet.org.cn/tjxx/3101</a> Jaipur Metro annual reports	Feb. 2020
Kazan (Russia)	<a href="https://transport.rajasthan.gov.in/jmrc/">https://transport.rajasthan.gov.in/jmrc/</a> International Metro Association reports	Feb. 2020
Kaohsiung (Taiwan)	<a href="http://eng.asmetro.ru/metro/techno_ekonom/">http://eng.asmetro.ru/metro/techno_ekonom/</a> Kaohsiung Rapid Transit Corp. transport volume statistics	Feb. 2020
Lausanne (Switzerland)	<a href="https://corp.krtc.com.tw/eng/News/annual_report">https://corp.krtc.com.tw/eng/News/annual_report</a> Transports Lausanne Annual Reports	Feb.2020
Lima (Peru)	<a href="http://app.iqr.ch/rapportactivite2015">http://app.iqr.ch/rapportactivite2015</a> Ministerio de Transportes y Comunicaciones Perú	Feb.2020
Mashhad (Iran)	<a href="https://portal.mtc.gob.pe/estadisticas">https://portal.mtc.gob.pe/estadisticas</a> Mashhad Urban Railway Corp. planning and development	Feb. 2020
Mumbai (India)	<a href="http://metro.mashhad.ir/">http://metro.mashhad.ir/</a> Mumbai Metro One Pvt. Ltd. right to information request	Feb. 2020
Nanning (China)	<a href="http://www.reliancemumbaimetro.com">http://www.reliancemumbaimetro.com</a> China Association of Metros annual reports	Feb. 2020
Naha (Japan)	<a href="https://www.camet.org.cn/tjxx/3101">https://www.camet.org.cn/tjxx/3101</a> Okinawa Ciy Monorail Line (Yui Rail)	Feb. 2020
Nanchang (China)	<a href="https://www.yui-rail.co.jp/yuirail/past-users/">https://www.yui-rail.co.jp/yuirail/past-users/</a> China Association of Metros annual reports	Feb. 2020
Ningbo (China)	<a href="https://www.camet.org.cn/tjxx/3101">https://www.camet.org.cn/tjxx/3101</a> China Association of Metros annual reports	Feb. 2020

Continued on next page

**Table A.1 – continued from previous page**

City	Source & URL	Date accessed
Palma (Spain)	Instituto Nacional de Estadística España <a href="https://www.ine.es/jaxiT3/Tabla.htm?t=20193">https://www.ine.es/jaxiT3/Tabla.htm?t=20193</a>	Feb. 2020
Panama City (Panama)	Instituto Nacional de Estadísticas y Censo Panamá <a href="https://www.inec.gob.pa/archivos/P053342420200113130756Cuadro%2018.pdf">https://www.inec.gob.pa/archivos/P053342420200113130756Cuadro%2018.pdf</a>	Feb. 2020
Porto (Portugal)	Statistics Portugal, Light rail (metro) survey <a href="https://www.ine.pt/xportal/xmain?xpid=INE&amp;xpgid=ine_base_dados">https://www.ine.pt/xportal/xmain?xpid=INE&amp;xpgid=ine_base_dados</a>	Feb. 2020
Qingdao (China)	China Association of Metros annual reports <a href="https://www.camet.org.cn/tjxx/3101">https://www.camet.org.cn/tjxx/3101</a>	Feb. 2020
Salvador da Bahia (Brazil)	Companhia de Transportes do Estado da Bahia <a href="http://www.ctb.ba.gov.br/modules/conteudo/conteudo.php?conteudo=29">http://www.ctb.ba.gov.br/modules/conteudo/conteudo.php?conteudo=29</a>	Feb. 2020
San Juan Puerto Rico (USA)	Instituto de Estadísticas de Puerto Rico <a href="https://indicadores.pr/dataset/numero-de-pasajeros-del-tren-urbano">https://indicadores.pr/dataset/numero-de-pasajeros-del-tren-urbano</a>	Feb. 2020
Santo Domingo (DR)	Oficina para el Reordenamiento del Transporte <a href="https://www.opret.gob.do/transparencia/estadisticasInstitucionales">https://www.opret.gob.do/transparencia/estadisticasInstitucionales</a>	Feb. 2020
Seattle (USA)	Sound Transit performance reports (Only Central Link Line) <a href="http://www.soundtransit.org/get-to-know-us/documents-reports/service-planning-ridership">www.soundtransit.org/get-to-know-us/documents-reports/service-planning-ridership</a>	Feb. 2020
Seville (Spain)	Instituto Nacional de Estadística España <a href="https://www.ine.pt/xportal/xmain?xpid=INE&amp;xpgid=ine_base_dados">https://www.ine.pt/xportal/xmain?xpid=INE&amp;xpgid=ine_base_dados</a>	Feb. 2020
Shenzhen (China)	China Association of Metros annual reports <a href="https://www.camet.org.cn/tjxx/3101">https://www.camet.org.cn/tjxx/3101</a>	Feb. 2020
Shenyang (China)	China Association of Metros annual reports <a href="https://www.camet.org.cn/tjxx/3101">https://www.camet.org.cn/tjxx/3101</a>	Feb. 2020
Suzhou, Jiangsu (China)	China Association of Metros annual reports <a href="https://www.camet.org.cn/tjxx/3101">https://www.camet.org.cn/tjxx/3101</a>	Feb. 2020
Turin (Italy)	Gruppo Torinese Transporti reports	Jul. 2017

Continued on next page

---

---

**Table A.1 – continued from previous page**

City	Source & URL	Date accessed
Valparaiso (Chile)	<a href="http://www.gtt.to.it/cms/notizie-eventi-e-informazioni">http://www.gtt.to.it/cms/notizie-eventi-e-informazioni</a> Memoria Anual Metro Valparaiso	Feb. 2020
Wuxi (China)	<a href="https://www.efe.cl/corporativo/documentos/memorias-anuales/metro-valparaiso/">https://www.efe.cl/corporativo/documentos/memorias-anuales/metro-valparaiso/</a> China Association of Metros annual reports	Feb. 2020
Xi'an, Shaanxi (China)	<a href="https://www.camet.org.cn/tjxx/3101">https://www.camet.org.cn/tjxx/3101</a> China Association of Metros annual reports	Feb. 2020
Zhengzhou (China)	<a href="https://www.camet.org.cn/tjxx/3101">https://www.camet.org.cn/tjxx/3101</a> China Association of Metros annual reports	Feb. 2020

---

---

*Note:* We were not able to obtain ridership data from the time of opening for the following 16 cities in the sample: Algiers (Algeria), Brasilia (Brazil), Bursa (Turkey), Chengdu (China), Chongqing (China), Dalian (China), Isfahan (Iran), Izmir (Turkey), Kunming (China), Maracaibo (Venezuela), Nanjing (China), Rennes (France), Shiraz (Iran), Tabriz (Iran), Valencia (Venezuela), and Wuhan (China).

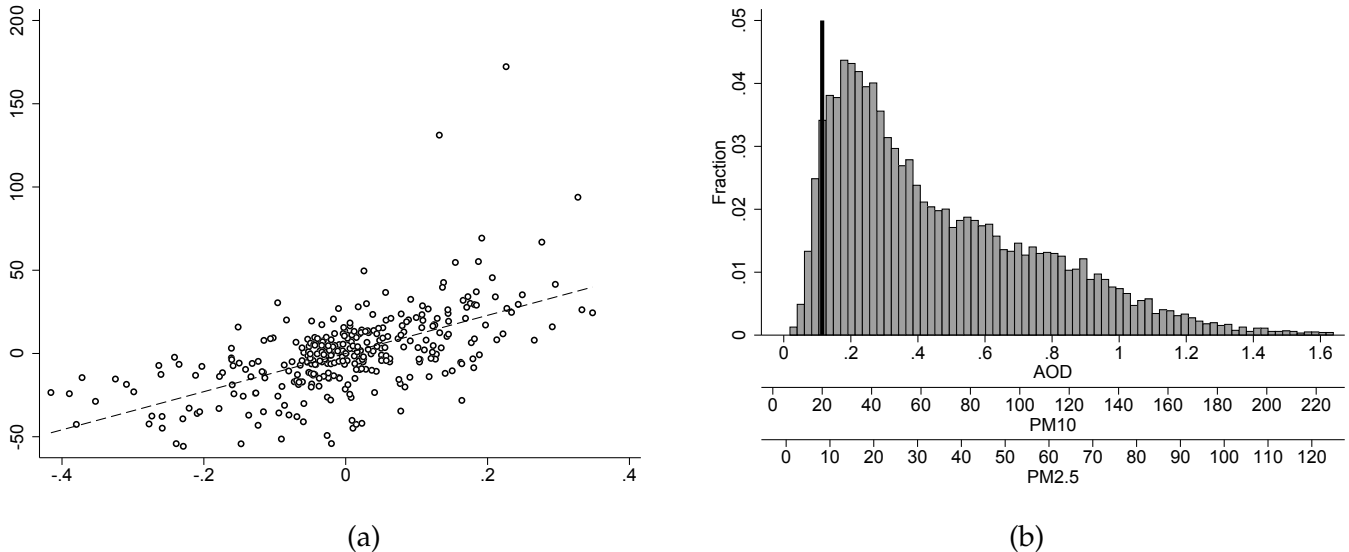
### C AOD vs ground based measurements

Table A.2: Relationship between AOD and Ground-based Particulate Measures

	PM10						PM2.5	
	(1)	(2)	(3)	(4)	(5)	(6)	(7)	(8)
AOD	135.8 (9.7)	114.6 (11.8)	118.1 (11.5)	113.0 (11.9)	101.7 (10.0)	103.3 (10.9)	76.6 (6.7)	60.6 (8.3)
cons	4.5 (2.8)	134.5 (39.3)	110.7 (39.8)	136.9 (39.5)	136.6 (41.1)	140.0 (42.3)	-0.5 (1.5)	19.9 (27.5)
Mean dep. var.	57.25	57.25	57.25	57.25	57.35	57.35	23.72	23.72
Mean ind. var.	0.39	0.39	0.36	0.39	0.37	0.39	0.32	0.32
$R^2$	0.50	0.82	0.81	0.82	0.83	0.82	0.61	0.85
N	340	340	340	340	339	339	217	217

Note: (1) Terra 10k disk, no controls. (2) Terra 10k disk, controls. (3) Aqua 10k disk, controls. (4) Terra 10k footprint, controls. (5) Terra 25k disk, controls. (6) Terra 25k footprint, controls. (7) Terra 10k disk, no controls. (8) Terra 10k disk, controls. Controls: continent-year indicators, average pixel count, and linear and quadratic terms in average temperature, precipitation, cloud cover, vapor pressure and frost days. Robust standard errors in parentheses.

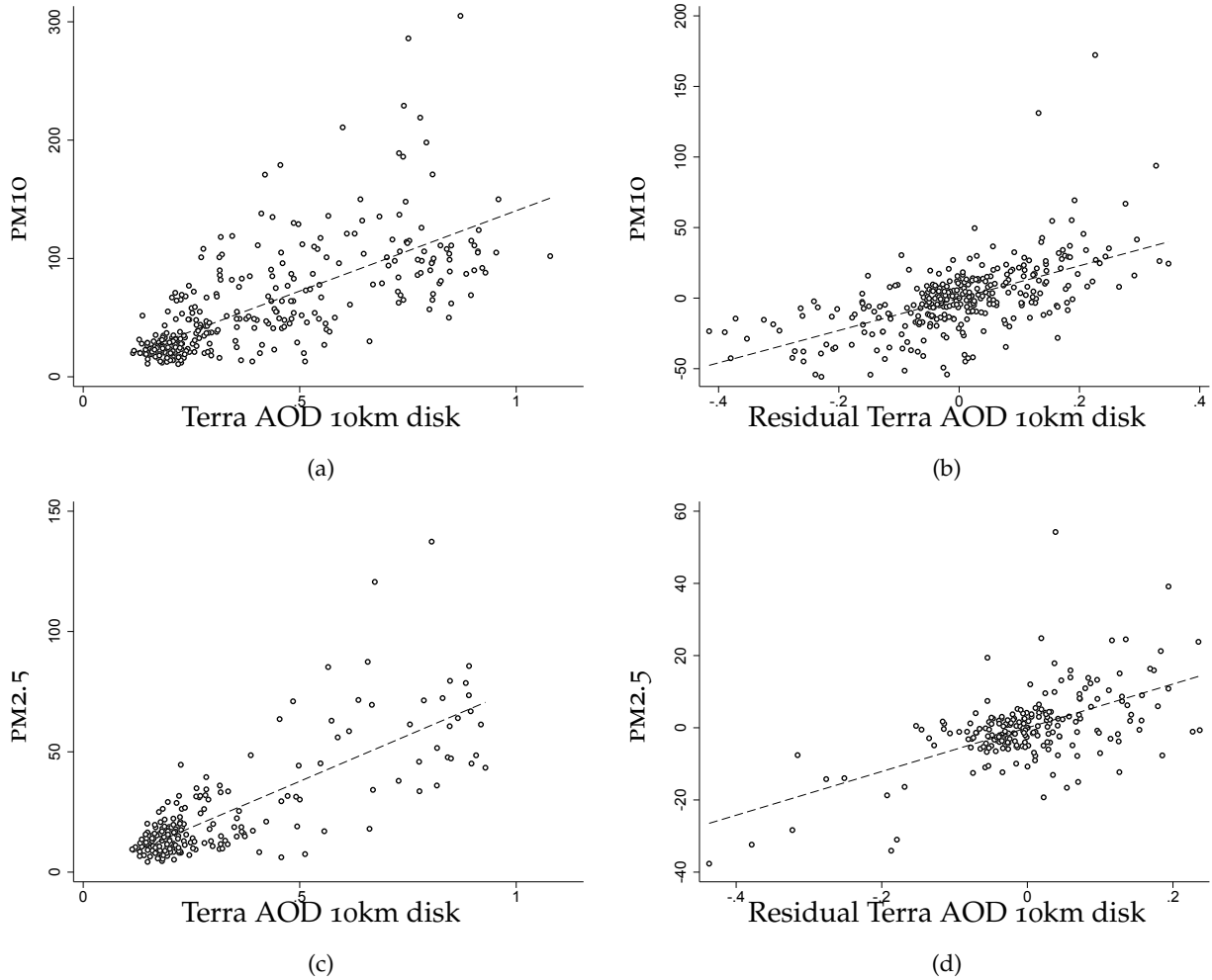
Figure A.2: AOD versus PM



Note: (a) Plot showing residualized PM<sub>10</sub> and AOD, together with linear trend. (b) Histogram of city-months by AOD, PM<sub>10</sub> and PM<sub>2.5</sub>. PM<sub>10</sub> and PM<sub>2.5</sub> axes rescaled from AOD using columns 1 and 4 of Table A.2. Black vertical line indicates WHO threshold level for annual average PM<sub>10</sub> exposure (WHO, 2006).

A series of papers have compared measures of AOD to measures of particulate concentration from surface instruments (e.g. Gupta, Christopher, Wang, Gehrig, Lee, and Kumar, 2006, Kumar,

Figure A.3: Plots of ground-based PM10 and PM2.5 vs. MODIS AOD



Note: Panel (a) Plot of ground-based PM10 against Terra MODIS AOD in a 10km disk. Panel (b) Plot of ground-based PM10 residual against Terra MODIS AOD in a 10km disk residual. Panel (c) Plot of ground-based PM2.5 against Terra MODIS AOD in a 10km disk. Panel (d) Plot of ground-based PM2.5 residual against Terra MODIS AOD in a 10km disk residual. NB: Scales not constant across graphs.

Chu, and Foster, 2007, Kumar, Chu, Foster, Peters, and Willis, 2011). In particular, Kumar *et al.* (2007) examines the ability of AOD to predict particulates in a set of large cities, several of which are subway cities. AOD is a good measure of airborne particulates, with two caveats. First, satellite reports of AOD describe daytime average conditions over a wide area at the particular time the satellite passes overhead, while ground based instruments record conditions at a particular location over a longer period. This naturally causes satellite and ground based measures to diverge. Second, ground based instruments report the concentration of dry particulates, while the satellite based measure has trouble distinguishing water vapor from other particles. This motivates the use of flexible climate controls in our analysis.

As a direct check on our AOD data, we use World Health Organization data (WHO, 2016a) describing average annual PM10 and PM2.5 concentrations ( $\mu\text{g}/\text{m}^3$ ) in cities where ground-based pollution readings were available. We successfully match 150 such cities with ground-based PM10 readings to our subway cities data. Of the 150, 79 report PM10 readings during three years, 32 during two years, and 39 in only one year. The readings span the 2007-2014 period, and not

all city-years record both PM<sub>10</sub> and PM<sub>2.5</sub>. Averaging monthly AOD values to calculate yearly averages, we obtain 340 comparable city-years for PM<sub>10</sub> and 217 comparable city-years for PM<sub>2.5</sub>. Note the limited amount of data available from ground-based instruments. Satellite data solve the issue of data scarcity. In particular, note that the ground based measurements are annual, as opposed to the monthly data we use elsewhere.

To compare the WHO ground-based annual measures of particulates to annual averages of MODIS AOD measurements in subway cities, we estimate the following regressions

$$PM_{yit} = \alpha_0 + \alpha_1 AOD_{it} + \text{controls}_{it} + \epsilon_{it},$$

where  $y \in \{2.5, 10\}$  is particulate size,  $i$  refers to cities and  $t$  to years for which we can match WHO data to our AOD sample.

Table A.2 reports results. The upper first column presents the results of a regression of the WHO measure of PM<sub>10</sub> on annual average Terra AOD within 10km of a subway city center. There is a strong positive relationship between the two quantities and the  $R^2$  of the regression is 0.50. The AOD coefficient of 135.81 in Column 1 means that a one unit increase in AOD maps to a 135.81  $\mu\text{g}/\text{m}^3$  increase in PM<sub>10</sub>. From Table 1 in the paper, we see that Terra 10k readings for North America decreased by 0.03 in subway cities between 2000 and 2017. Multiplying by 135.81 gives a 4.1  $\mu\text{g}^3$  decrease in PM<sub>10</sub>. By contrast, according to US EPA historical data, during this same period US average PM<sub>10</sub> declined from 64.7 to 57.7  $\mu\text{g}/\text{m}^3$ , or about a 7 unit decrease.<sup>3</sup> Since Table 1 in the paper reports AOD for just the three cities in North America with new subways, while the EPA reports area weighted measures for the US, this seems as close as could be expected.

In Column 2, we conduct the same regression but include linear and quadratic terms in our climate variables, average pixel count, and continent-year indicators. The coefficient on AOD drops from 135.81 to 114.60, and the  $R^2$  increases to 0.82. In Column 3, we conduct exactly the same regression, but rely on AOD measurements from the Aqua satellite. As expected this leaves our estimates qualitatively unchanged.

Columns (4)-(6) repeat (2) but use different geographies to construct the AOD measure. In Column (4) we measure AOD in the intersection of the lights based city footprint and a 10km disk centered on the city. In Column (5) we measure AOD in a 25km disk centered on the city. In Column (6) we measure AOD in the intersection of the lights based footprint and the 25km disk. Coefficients vary slightly over the different specifications, but  $R^2$ s do not. In theory, this sequence of regressions could have revealed that ground based instruments are more closely related to a particular AOD measure. In fact, this seems not to be the case. Thus, the comparison of remotely sensed and ground based measures does not suggest that footprints are to be preferred to disks for the analysis based on  $R^2$ s. Given this, and given that most subway systems concentrate their service in the center part of the city (Gonzalez-Navarro and Turner, 2018), we rely on AOD calculated of centrally located 10km disks for our main analysis.

For completeness, columns (7) and (8) replicate columns (1) and (2), but use ground based measures of PM<sub>2.5</sub> as the dependent variable. Since PM<sub>2.5</sub> comprises a smaller fraction of all airborne particulates than does PM<sub>10</sub>, the smaller coefficients in these regressions is expected. In fact, the AOD coefficient for PM<sub>2.5</sub> from Column (8) is about 53% of the one for PM<sub>10</sub> in Column (2). This is consistent with the PM<sub>10</sub> to PM<sub>2.5</sub> conversion factors used by the World Health Organisation (WHO, 2016a).<sup>4</sup>

All specifications reported in Table A.2 assume a linear relationship between AOD and PM. Figure A.2(a) plots residuals of regressions of PM<sub>10</sub> and AOD on all controls used in Column 2

<sup>3</sup><https://www.epa.gov/air-trends/particulate-matter-pm10-trends>, accessed July 2, 2020.

<sup>4</sup>We note that the results in Table A.2 are quite different from those on which the 2013 Global burden of disease estimates are based (Brauer *et al.* 2015). In particular, they estimate

$$\ln(\text{PM}_{2.5}) \approx 0.8 + 0.7 \ln(\text{AOD}).$$

of Table A.2, along with a linear regression line. This graph illustrates both how closely the two variables track each other and how close to linear is the relationship between them.

Recall that the ground-based instruments and MODIS, in fact, measure something different. Ground-based instruments measure pollution at a point over an extended period of time. Remote sensing measures particulates across a wide area at an instant. Given this difference, the extent to which the two measures agree seems remarkable.

In addition to validating the use of remotely sensed AOD, Table A.2 provides a basis for translating our estimates of the relationship between subways and AOD into a relationship between subways and  $\text{PM}_{2.5}$ , or  $\text{PM}_{10}$ . To illustrate this process, and to help to describe our data, Figure A.2(b) provides a histogram of the 21,806 city-months used for our main econometric analysis. The figure provides three different scales for the horizontal axis. The top scale is the raw AOD measure. The second two axes are affine transformations of the AOD scale into  $\text{PM}_{10}$  and  $\text{PM}_{2.5}$  based on columns (1) and (7) of Table A.2. For reference, the black line in the figure gives the World Health Organization recommended maximum annual average  $\text{PM}_{10}$  exposure level ( $20 \mu\text{g}/\text{m}^3$ ).

#### D Global Burden of Disease based mortality estimates

The integrated risk functions in Burnett *et al.* (2014) express the likelihood of dying from a disease at current  $\text{PM}_{2.5}$  exposure, relative to an environment where  $\text{PM}_{2.5}$  concentrations are set to a baseline harmless level of exposure. If  $D_d$  is the event of dying from disease  $d$ , the risk ratio (RR) of being exposed to  $\text{PM}_{2.5}$  concentration  $c$  is given by  $RR_d(c, \bar{c}) = P(D_d | c) / P(D_d | \bar{c})$ , where  $\bar{c}$  denotes the baseline harmless concentration. Burnett *et al.* (2014) model  $RR_d(c, \bar{c})$  to exhibit diminishing marginal risk:  $RR(c, \bar{c}) = 1 + \alpha(1 - e^{-\gamma(c - \bar{c})^\delta})$  if  $c > \bar{c}$ , and  $RR(c, \bar{c}) = 1$  otherwise, with  $\bar{c}$  assumed to lie uniformly between  $5.8$  and  $8.8 \mu\text{g}/\text{m}^3$ . We refer the reader to Burnett *et al.* (2014) for details regarding the parametrization and estimation of these functions for each disease.

As described in the main text, we obtain RR functions for five diseases: ischemic heart disease, cerebrovascular disease (stroke), chronic obstructive pulmonary disease, lung cancer, and lower respiratory infection. For deaths attributable to stroke and ischemic heart disease, the integrated risk functions are age-specific. To construct population attributable fractions (PAF) for every disease and, when applicable, every age-group, we first predict pre and post-subway  $\text{PM}_{2.5}$  concentrations using the regression specification in Column 8 of Table A.2. Specifically, we obtain predicted  $\text{PM}_{2.5}$  values from the annual city average of AOD (and all other covariates) during the 12 months preceding the subway opening. The post-subway  $\text{PM}_{2.5}$  concentrations are obtained by subtracting  $0.028 \times 60.57 = 1.696 \mu\text{g}/\text{m}^3$  to the pre-subway concentration, where  $0.028$  is the subway AOD effect from Table 4 in the paper, and  $60.57$  is the AOD coefficient in Column 8 of Table A.2.

Let  $c_0$  and  $c_1$  respectively denote the pre and post-subway  $\text{PM}_{2.5}$  concentrations in a given city. For the purpose of our burden of disease calculations, the relevant risk ratio is  $RR_d(c_1, c_0) = P(D_d | c_1) / P(D_d | c_0)$ . Using the  $RR_d(c, \bar{c})$  functions in Burnett *et al.* (2014), we obtain this number by computing  $RR_d(c_1, c_0) = RR_d(c_1, \bar{c}) / RR_d(c_0, \bar{c})$ . Here,  $RR_d(c_1, c_0)$  expresses how much less likely

---

Comparing with Table A.2, we see that these coefficient estimates are quite different. The difference reflects primarily our use of the level of  $\text{PM}_{2.5}$ , rather than its logarithm, as the dependent variable. We also use the level of AOD rather than its logarithm as the explanatory variable. Since AOD is typically around  $0.5$ , this turns out not to be important. Finally, our sample describes a different and more urban sample of locations, relies on annual rather than daily data, and measures AOD using just MODIS data rather than an average of MODIS and a measure imputed using a climate model and ground based emissions release information. We prefer the formulation in Table A.2 to that in Brauer *et al.* (2015) for three reasons. First, AOD is already a logarithm (see footnote 4 in the paper), so the Brauer *et al.* specification uses the logarithm of a logarithm as its main explanatory variable. Second, mortality and morbidity estimates are typically based on levels of pollutants, not on percentage changes, so the dependent variable in our regressions is more immediately useful for evaluating the health implications of changes in AOD. Finally, we control for weather conditions, which appears to be important. In any case, the  $R^2$  in both studies is of similar magnitude.

it is that individuals die of disease  $d$  when exposed to concentration  $c_1$ , relative to concentration  $c_0$ . Assuming that 100% of the city population is exposed to  $c_0$  and then  $c_1$ , the population attributable fraction is then just  $PAF_d = 1 - RR_d(c_1, c_0) = 1 - P(D_d | c_1) / P(D_d | c_0)$ . Interpreting  $P(D_d | c)$  as the fraction of the total population that died of disease  $d$  when exposed to PM2.5 concentration  $c$ , we find that  $PAF_d$  represents the fraction of total deaths from  $d$  that occurred because of incremental pollution  $c_1 - c_0$ .

Finally, for each high AOD city  $i$ , we calculate the number of death attributable to disease  $d$  in age-group  $a$  (denoted  $M_{ida}$  below). We use disease-specific country-level death rates from the World Health Organisation (WHO, 2016c) and apply them to city populations. Mortality data from the WHO is only available in 2000, 2005, 2010, and 2015. We use the year closest to a city's subway opening year. The total number of avoided death in city  $i$  is given by  $\sum_d \sum_a PAF_{ida} \cdot M_{ida}$ .

## E Supplemental Tables

Table A.3: Average Effect of Subway Openings: Robustness Checks

	(1)	(2)	(3)	(4)	(5)	(6)
post	-0.0094 (0.0090)	-0.0035 (0.0085)	-0.0093 (0.0090)	-0.0080 (0.0088)	-0.0050 (0.0088)	-0.0082 (0.0086)
satellite	Y	Y	Y	Y	Y	Y
cont. $\times$ year	Y	Y	Y	Y	Y	Y
city $\times$ cal. mo.	Y	Y	Y	Y	Y	Y
climate $\times$ cont.	Y	Y	Y	Y	Y	Y
Mean AOD	0.46	0.41	0.45	0.46	0.45	0.47
$R^2$	0.80	0.87	0.84	0.79	0.80	0.80
# events	58	58	58	58	58	58
# cities	58	58	58	58	58	58
N	21806	21806	19635	21702	22605	22497

*Note: Dependent variable is mean AOD in a 10km disk with centroid in the city center unless noted otherwise below. (1) Replicates Column 5 from Table 2 in the paper (for reference). (2) Same as (1) but weight observations by pixel count. (3) Same as (1) but drop observations with low pixel count. (4) Same as (1) but calculating AOD in city footprint within 10km from the city center. (5) Same as (1) but calculating AOD in a 25km disk centered around the city center. (6) Same as (1) but calculating AOD in city footprint within 25km from the city center. All specifications control for city fixed effects, city-specific pre-window indicators, city-specific post-window indicators, and city-specific period-0 indicators. Climate controls are pixel count and linear and quadratic terms in temperature, precipitation, cloud cover, vapor pressure and frost days. Standard errors clustered at the city level in parentheses.*

Table A.4: Average Effect of Subway Openings: Different Window of Analysis

	(1)	(2)	(3)	(4)	(5)
post	-0.0094 (0.0090)	-0.0027 (0.0108)	-0.0040 (0.0096)	-0.0008 (0.0084)	-0.0057 (0.0088)
satellite	Y	Y	Y	Y	Y
cont. $\times$ year	Y	Y	Y	Y	Y
city $\times$ cal. mo.	Y	Y	Y	Y	Y
climate $\times$ cont.	Y	Y	Y	Y	Y
Mean AOD	0.46	0.46	0.46	0.44	0.45
$R^2$	0.80	0.80	0.81	0.81	0.81
# events	58	64	60	55	44
# cities	58	64	60	55	44
N	21806	24028	22580	20684	16422

*Note: Dependent variable is mean AOD in a 10km disk centered around the city center. (1) Column 5, Table 2 in the paper (for reference). (2) Same as (1) but treatment and control window are 6 months. (3) Same as (1) but treatment and control window are 12 months. (4) Same as (1) but treatment and control window are 24 months. (5) Same as (1) but treatment and control window are 36 months. All specifications control for city fixed effects, city-specific pre-window indicators, city-specific post-window indicators, and city-specific period-0 indicators. Climate controls are pixel count and linear and quadratic terms in temperature, precipitation, cloud cover, vapor pressure and frost days. Standard errors clustered at the city level in parentheses.*

Table A.5: Effect of Subway Openings in High AOD Cities: Robustness Checks

	(1)	(2)	(3)	(4)	(5)	(6)	(7)	(8)	(9)	(10)
post	-0.0295 (0.0157)	-0.0320 (0.0134)	-0.0305 (0.0145)	-0.0321 (0.0129)	-0.0258 (0.0142)	-0.0254 (0.0124)	-0.0134 (0.0152)	-0.0238 (0.0110)	-0.0219 (0.0147)	-0.0286 (0.0108)
satellite	Y	Y	Y	Y	Y	Y	Y	Y	Y	Y
cont. $\times$ year	Y	Y	Y	Y	Y	Y	Y	Y	Y	Y
city $\times$ cal. mo.	Y	Y	Y	Y	Y	Y	Y	Y	Y	Y
climate $\times$ cont.	Y	Y	Y	Y	Y	Y	Y	Y	Y	Y
Mean AOD	0.63	0.43	0.66	0.42	0.67	0.43	0.66	0.41	0.68	0.43
bootstrap p-value	0.102	0.028	0.046	0.028	0.091	0.049	0.389	0.045	0.146	0.014
$R^2$	0.77	0.84	0.70	0.79	0.65	0.74	0.63	0.79	0.66	0.77
# events	29	29	29	29	29	29	29	29	29	29
# cities	29	490	29	489	29	486	29	491	29	487
N	10896	183548	9820	165235	10894	179065	11411	190020	11361	184165

Note: Dependent variable is mean AOD in a 10km disk centered around the city center unless noted otherwise below. Columns (1-2) replicate columns 5 and 6 in Table 4, but weight observations by pixel count. (3-4) Same as Columns 5 and 6 in Table 4, but drop observations with low pixel count. (5-6) Same as Columns 5 and 6 in Table 4, but calculating AOD in city footprint within 10km from the city center. (7-8) Same as Columns 5 and 6 in Table 4, but calculating AOD in a 25km disk centered around the city center. (9-10) Same as Columns 5 and 6 in Table 4, but calculating AOD in city footprint within 25km from the city center. All specifications control for city fixed effects, city-specific pre-window indicators, city-specific post-window indicators, and city-specific period-0 indicators. Climate controls are pixel count and linear and quadratic terms in temperature, precipitation, cloud cover, vapor pressure and frost days.

Table A.6: Average Effect of Subway Openings in high AOD cities: Different Window Widths

	(1)	(2)	(3)	(4)	(5)	(6)	(7)	(8)	(9)	(10)
post	-0.0270 (0.0147)	-0.0284 (0.0130)	-0.0032 (0.0212)	0.0012 (0.0215)	-0.0144 (0.0164)	-0.0121 (0.0158)	-0.0116 (0.0131)	-0.0160 (0.0109)	-0.0185 (0.0136)	-0.0215 (0.0099)
satellite	Y	Y	Y	Y	Y	Y	Y	Y	Y	Y
cont. × year	Y	Y	Y	Y	Y	Y	Y	Y	Y	Y
city × cal. mo.	Y	Y	Y	Y	Y	Y	Y	Y	Y	Y
climate × cont.	Y	Y	Y	Y	Y	Y	Y	Y	Y	Y
Mean AOD	0.66	0.43	0.66	0.43	0.66	0.43	0.64	0.42	0.66	0.42
bootstrap p-value	0.083	0.049	0.863	0.952	0.374	0.436	0.381	0.150	0.170	0.046
R <sup>2</sup>	0.66	0.75	0.66	0.75	0.66	0.75	0.70	0.75	0.68	0.75
# events	29	29	29	29	29	29	27	27	22	22
# cities	29	490	29	490	29	490	27	488	22	483
N	10896	183548	10896	183548	10896	183548	10169	182821	8201	180853

Note: Dependent variable is mean AOD in a 10km disk centered around the city center. (1-2) Same as Columns 5 and 6 in Table 4 (for reference). (3-4) Same as (1-2) but treatment and control window are 6 months. (5-6) Same as (1-2) but treatment and control window are 12 months. (7-8) Same as (1-2) but treatment and control window are 24 months. (9-10) Same as (1-2) but treatment and control window are 36 months. All specifications control for city fixed effects, city-specific pre-window indicators, city-specific post-window indicators, and city-specific period-0 indicators. Climate controls are pixel count and linear and quadratic terms in temperature, precipitation, cloud cover, vapor pressure and frost days. Standard errors clustered at the city level in parentheses.

Table A.7: City Level Descriptive Statistics

City	Plan approved	Construction begins	Opening date	Stations added			Daily ridership	Mean AOD	SD AOD	City population	Country GDP PC
				opening	1st exp.	2nd exp.					
Rennes (France)	1989	Jan. 1997	Mar. 2002	15	n.a.	n.a.	n.a.	0.20	0.10	283	33,534
Bursa (Turkey)	1997	Jan. 1998	Aug. 2002	17	n.a.	n.a.	n.a.	0.26	0.09	1,290	10,544
Copenhagen (Denmark)	1995	Nov. 1996	Nov. 2002	11	n.a.	n.a.	87,811	0.16	0.08	1,089	34,706
Porto (Portugal)	1996	Mar. 1999	Dec. 2002	8	6	7	35,200	0.18	0.08	1,264	23,297
Delhi (India)	1995	Jan. 1998	Dec. 2002	6	3	22	184,000	0.74	0.29	16,956	2,144
Dalian (China)	1999	Sep. 2000	May 2003	12	6	17	n.a.	0.54	0.23	3,338	4,993
Naha (Japan)	1996	Nov. 1996	Aug. 2003	15	n.a.	n.a.	31,237	0.29	0.15	306	34,120
Tianjin (China)	1984	Jan. 2001	Mar. 2004	7	25	17	n.a.	0.64	0.24	7,901	5,239
Gwangju (South Korea)	1994	Aug. 1996	Apr. 2004	13	n.a.	n.a.	36,780	0.41	0.22	1,388	25,527
Wuhan (China)	1999	Dec. 2000	Sep. 2004	25	20	13	n.a.	0.87	0.28	7,036	5,461
Shenzhen (China)	1992	Dec. 1998	Dec. 2004	18	69	13	249,722	0.76	0.28	8,087	5,572
San Juan Puerto Rico (USA)	1992	Jul. 1996	Apr. 2005	16	n.a.	n.a.	24,000	0.22	0.11	2,495	49,527
Chongqing (China)	1983	Dec. 2000	Jun. 2005	13	12	16	n.a.	0.91	0.25	9,293	5,900
Kazan (Russia)	1989	Aug. 1997	Aug. 2005	5	n.a.	n.a.	53,055	0.22	0.15	1,117	13,581
Nanjing (China)	1994	Dec. 2000	Aug. 2005	13	3	29	n.a.	0.77	0.29	5,076	6,010
Valparaiso (Chile)	1999	May 2002	Nov. 2005	20	n.a.	n.a.	32,755	0.10	0.03	842	13,324
Turin (Italy)	1999	Dec. 2000	Feb. 2006	11	n.a.	n.a.	38,275	0.26	0.13	1,707	33,214
Daejon (South Korea)	1996	Jan. 1996	Mar. 2006	12	n.a.	n.a.	68,939	0.38	0.23	1,437	27,555
Valencia (Venezuela)	1994	Nov. 1997	Nov. 2006	3	n.a.	n.a.	n.a.	0.23	0.11	1,548	11,531
Maracaibo (Venezuela)	1998	Mar. 2004	Nov. 2006	2	n.a.	n.a.	n.a.	0.28	0.13	1,707	11,531
Kaohsiung (Taiwan)	1994	Jan. 2001	Mar. 2008	23	13	n.a.	122,243	0.54	0.21	1,508	38,122
Palma (Spain)	2004	Aug. 2005	Jul. 2008	9	6	n.a.	4,374	0.18	0.06	375	34,865
Lausanne (Switzerland)	2000	Feb. 2004	Oct. 2008	14	n.a.	n.a.	66,852	0.19	0.07	356	54,124
Santo Domingo (DR)	2005	Nov. 2005	Jan. 2009	16	13	n.a.	62,293	0.30	0.15	2,480	10,075

Continued on next page

Table A.7 – continued from previous page

City	Plan approved	Construction begins	Opening date	Stations added			Daily ridership	Mean AOD	SD AOD	City population	Country GDP PC
				opening	1st exp.	2nd exp.					
Adana (Turkey)	1988	Sep. 1996	Mar. 2009	8	n.a.	n.a.	n.a.	0.33	0.12	1,453	16,317
Seville (Spain)	1999	Aug. 2005	Apr. 2009	17	n.a.	n.a.	43,461	0.20	0.08	694	34,496
Seattle (USA)	1996	Nov. 2003	Jul. 2009	8	n.a.	n.a.	15,437	0.17	0.08	3,017	49,706
Dubai (UAE)	2005	Mar. 2006	Sep. 2009	10	16	n.a.	169,816	0.51	0.24	1,699	65,788
Chengdu (China)	2000	Dec. 2005	Sep. 2010	16	20	5	n.a.	0.90	0.32	7,481	9,131
Shenyang (China)	1999	Nov. 2005	Sep. 2010	22	19	n.a.	434,428	0.48	0.26	5,819	9,131
Xian, Shaanxi (China)	1994	Sep. 2006	Sep. 2011	17	26	n.a.	295,220	0.73	0.25	5,684	10,043
Bangalore (India)	2003	Apr. 2007	Oct. 2011	7	10	n.a.	18,436	0.47	0.12	8,579	4,461
Mashhad (Iran)	1994	Dec. 1999	Oct. 2011	21	6	n.a.	83,345	0.22	0.10	2,717	18,195
Algiers (Algeria)	1988	Mar. 1993	Nov. 2011	10	n.a.	n.a.	n.a.	0.33	0.17	2,461	13,342
Almaty (Kazakhstan)	1980	Sep. 1988	Dec. 2011	7	n.a.	n.a.	18,228	0.25	0.06	1,470	22,022
Lima (Peru)	1986	Oct. 1986	Apr. 2012	16	n.a.	n.a.	120,575	0.71	0.19	9,150	10,496
Suzhou, Jiangsu (China)	2002	Dec. 2007	Apr. 2012	24	20	38	196,778	0.81	0.25	4,326	10,365
Kunming (China)	2009	May 2010	Jun. 2012	2	12	18	n.a.	0.31	0.24	3,602	10,423
Hangzhou (China)	2005	Mar. 2007	Nov. 2012	31	13	10	390,595	0.79	0.22	6,112	10,568
Brescia (Italy)	2000	Jan. 2004	Mar. 2013	17	n.a.	n.a.	42,943	0.27	0.14	452	36,113
Harbin (China)	2005	Sep. 2009	Sep. 2013	17	n.a.	n.a.	182,333	0.30	0.18	5,457	11,041
Zhengzhou (China)	2008	Jun. 2009	Dec. 2013	20	15	20	244,722	0.83	0.34	4,074	11,189
Changsha (China)	2008	Sep. 2009	Apr. 2014	18	n.a.	n.a.	233,528	0.83	0.25	3,799	11,374
Panama City (Panama)	2009	Feb. 2011	Apr. 2014	12	n.a.	n.a.	223,661	0.33	0.14	1,615	18,887
Ningbo (China)	2003	Jun. 2009	May 2014	20	21	n.a.	104,889	0.81	0.22	3,187	11,420
Mumbai (India)	2004	Feb. 2008	Jun. 2014	12	n.a.	n.a.	260,000	0.59	0.35	18,992	5,095
Salvador da Bahia (Brazil)	1999	Apr. 2000	Jun. 2014	5	2	n.a.	42,782	0.20	0.07	3,517	15,231
Wuxi (China)	2006	Nov. 2009	Jul. 2014	24	18	n.a.	229,642	0.84	0.24	2,915	11,513
Shiraz (Iran)	1993	Jun. 2006	Oct. 2014	5	n.a.	n.a.	n.a.	0.27	0.09	1,513	15,816

Continued on next page

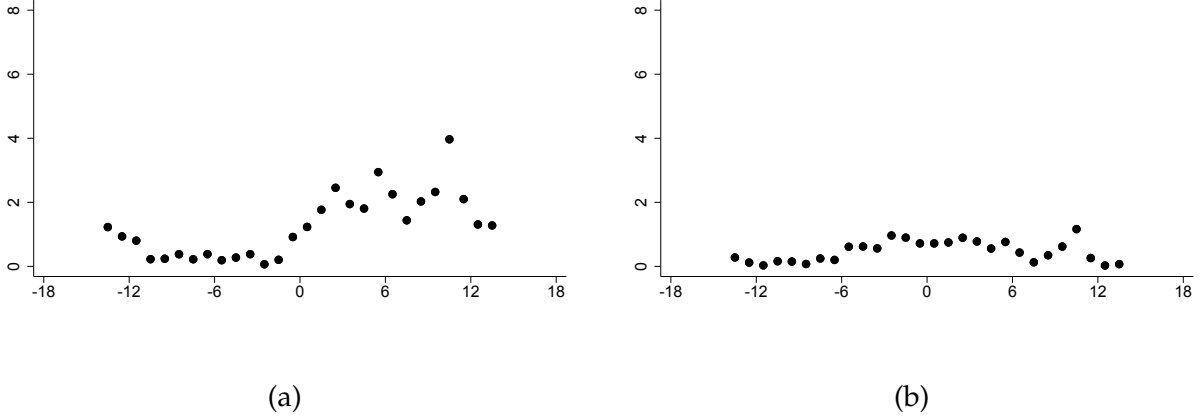
Table A.7 – continued from previous page

City	Plan approved	Construction begins	Opening date	Stations added		Daily ridership	Mean AOD	SD AOD	City population	Country GDP PC	
				opening	1st exp. 2nd exp.						
Chennai (India)	2008	Jun. 2009	Jun. 2015	6	n.a. n.a.	10,923	0.42	0.11	9,554	5,391	
Jaipur (India)	2010	Feb. 2011	Jun. 2015	9	n.a. n.a.	20,064	0.41	0.21	3,380	5,391	
Tabriz (Iran)	2000	n.a.	Aug. 2015	6	n.a. n.a.	n.a.	0.30	0.09	1,538	15,152	
Isfahan (Iran)	1996	Jun. 2001	Oct. 2015	10	n.a. n.a.	n.a.	0.40	0.10	1,901	14,994	
Nanchang (China)	2006	Jul. 2009	Dec. 2015	24	16	n.a.	304,894	0.79	0.25	3,053	12,034
Qingdao(China)	2009	Nov. 2009	Dec. 2015	9	18	n.a.	182,589	0.72	0.23	5,041	12,034
Dongguan (China)	2007	Mar. 2010	May 2016	15	n.a. n.a.	107,611	0.88	0.25	7,330	12,229	
Fuzhou (China)	2009	Dec. 2009	May 2016	9	n.a. n.a.	136,969	0.50	0.18	3,344	12,229	
Nanning (China)	2008	Dec. 2011	Jun. 2016	10	17	n.a.	269,808	0.85	0.30	3,353	12,268
Average	1999	Jan. 2004	Jun. 2010	13.8	16.0	17.3	130,528	0.47	0.32	4,028	17,755

Note: Daily ridership reported 18 months after opening. Mean and SD AOD columns report mean and standard deviation values in a 10km radius using Terra satellite monthly observations from 2000-2017. City population column reports metropolitan area population in thousands at time of subway opening. Country GDP PC reports PPP-adjusted country GDP per capita from Penn World Tables Version 9.1 reported at time of subway opening.

## F Supplemental Figures

Figure A.4: Structural Break Tests



Notes: (a) Plot of Wald statistics for tests of a regression intercept discontinuity at time  $\tau$ . Test statistics calculated in regressions that also control for a satellite indicator, year-by-continent indicator variables, city-by-calendar month indicators, and continent specific climate variables (AOD pixel count and linear and quadratic terms in temperature, precipitation, cloud cover, vapor pressure and frost days). (b) Plot of Wald statistics for tests of a trend break at time  $\tau$  conditional on a discontinuity in the mean level of AOD at  $\tau = 1$ . Other details are the same as in Panel (a).

The regressions underlying Figure 4(a) in the paper are,

$$AOD_{it} = \beta_i + \alpha_{1j}D_{it}(j,k) + \gamma'X_{it} + \epsilon_{it} \quad (1)$$

For our main analysis we set  $k = 18$ . This window length strikes a balance between maintaining the set of cities from which we identify our coefficient of interest and having a long analysis window. Thus, we use a 37 month study window and estimate Equation (1) for each month in  $j \in \{-14, \dots, 14\}$  with errors clustered at the city level. We then calculate a Wald test of  $\alpha_{1j} = 0$  for each  $j$ . Including pre- and post-period indicators in these regressions allows us to use all city-months in our sample to estimate city-by-calendar month indicators, continent-by-year indicators and climate variables, while only using AOD variation near the subway opening date to estimate the effect of subways on AOD. Here and throughout, we allow for city specific pre- and post-treatment windows. This extra flexibility helps to insure that we use the same variation in the data to estimate the subway effect, even as we change samples. We discuss this further below. Panel (a) of Figure 4 plots these test statistics.

The figure shows a clear pattern. Wald statistics increase from a low level to a peak between month 6 and 12 of subway opening. Andrews (2003) gives (asymptotic) critical values for the test statistic values we have just generated, a ‘sup-Wald’ test for  $\alpha_{1j} = 0$  for all  $j$ . For our case, where the break in question affects only one parameter and where we trim 25% from the boundaries of the sample, the 5% critical value of this statistic is 7.87, much greater than the largest value that we observe for the Wald statistic in the months after a system opening. With this said, our estimation framework differs from the one for which this test statistic is derived in several small ways, and so we regard this test with some caution. In conclusion, while we cannot reject a null of no level break in the overall sample, it is important to note that the plot suggests that whatever pollution reducing effects the subway system opening leads to occur in the months *after* the subway opens.

In Figure 4(b) in the paper we check for a change in the trend of AOD associated with subway openings. We proceed much as in our test for a break, but instead look for a change in trend around the time of a subway opening conditional on a level break at  $\tau = 1$ . Formally, this means estimating the following set of regressions,

$$AOD_{it} = \beta_i + \alpha_1 \tau_{it} + \alpha_2 \tau_{it} D_{it}(j,k) + \alpha_3 D_{it}(1,k) + \gamma' X_{it} + \epsilon_{it} \quad (2)$$

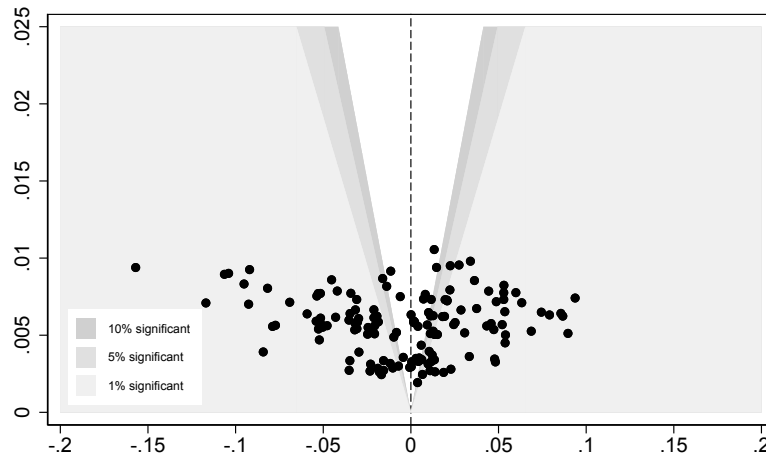
As before, we estimate the regression (2) for each month in  $j \in \{-14, \dots, 14\}$  with errors clustered at the city level and calculate the Wald test for  $\alpha_2 = 0$  for each regression.<sup>5</sup> Panel (b) of Figure 4 in the paper plots these Wald statistic values as  $j$  varies.<sup>6</sup> Thus, conditional on a step at  $\tau = 1$ , subway openings do not seem to cause a change in the trend of AOD in a city.

---

<sup>5</sup>An alternative would be to simultaneously search for locations of the break and trend break. Hansen (2000) argues that sequential searching, as we do, arrives at the same result.

<sup>6</sup>All values are well below the 10% critical value of 6.35 given in Andrews (2003). Again, our framework differs from the framework under which this test statistic is derived so this test should be regarded with caution.

Figure A.5: Heterogeneous treatment effects for all expansions.



*Note: Illustration of all event-specific subway expansion effects. Controls are as in Column 1 of Table 7 in the paper.  $x$  axis is the estimated treatment effect,  $y$  is the standard error of the estimated treatment effect. Region in white contains estimates that are not significantly different from zero. Dark, medium and light gray regions are different from zero at 10%, 5% and 1% in two-sided tests. Standard errors clustered at the event level.*

## References

- Andrews, Donald W.K. 2003. Tests for parameter instability and structural change with unknown change point: A corrigendum. *Econometrica* : 395–397.
- Brauer, Michael, Greg Freedman, Joseph Frostad, Aaron Van Donkelaar, Randall V. Martin, Frank Dentener, Rita van Dingenen, Kara Estep, Heresh Amini, and Joshua S. Apte. 2015. Ambient air pollution exposure estimation for the global burden of disease 2013. *Environmental Science & Technology* 50(1): 79–88.
- Burnett, Richard T *et al.* 2014. An integrated risk function for estimating the global burden of disease attributable to ambient fine particulate matter exposure. *Environmental Health Perspectives* 122(4): 397.
- Gonzalez-Navarro, Marco and Matthew A Turner. 2018. Subways and urban growth: Evidence from earth. *Journal of Urban Economics* 108: 85–106.
- Gupta, Pawan, Sundar A. Christopher, Jun Wang, Robert Gehrig, Yc Lee, and Naresh Kumar. 2006. Satellite remote sensing of particulate matter and air quality assessment over global cities. *Atmospheric Environment* 40: 5880–5892.
- Hansen, Bruce E. 2000. Testing for structural change in conditional models. *Journal of Econometrics* 97(1): 93–115.
- Kumar, Naresh, Allen Chu, and Andrew Foster. 2007. An empirical relationship between pm2.5 and aerosol optical depth in Delhi metropolitan. *Atmospheric Environment* 41: 4492–4503.
- Kumar, Naresh, Allen D. Chu, Andrew D. Foster, Thomas Peters, and Robert Willis. 2011. Satellite remote sensing for developing time and space resolved estimates of ambient particulate in Cleveland, OH. *Aerosol Science and Technology* 45: 1090–1108.
- World Health Organization. 2006. WHO air quality guidelines. Geneva: World Health Organization.
- World Health Organization. 2016a. Global urban ambient air pollution database. [http://www.who.int/phe/health\\_topics/outdoorair/databases/cities/en/](http://www.who.int/phe/health_topics/outdoorair/databases/cities/en/). Accessed: 2017-04-10.
- World Health Organization. 2016c. Global health estimates 2015: Deaths by cause, age, sex, by country and by region, 2000-2015.